

Life Cycle Assessment of Zero-Emission Magneto-Rheological Brake with Promising Environmental Performance Compared to Conventional Disc Brake

Original

Life Cycle Assessment of Zero-Emission Magneto-Rheological Brake with Promising Environmental Performance Compared to Conventional Disc Brake / Calvi, F., Accardo, A., De Carvalho Pinheiro, H., Imberti, G., Spessa, E., Carello, M.. - In: WORLD ELECTRIC VEHICLE JOURNAL. - ISSN 2032-6653. - 17:4(2026). [10.3390/wevj17040220]

Availability:

This version is available at: 11583/3010249 since: 2026-04-24T15:01:10Z

Publisher:

MDPI

Published

DOI:10.3390/wevj17040220

Terms of use:




This article is made available under terms and conditions as specified in the corresponding bibliographic description in the repository

Publisher copyright

(Article begins on next page)

Article

Life Cycle Assessment of Zero-Emission Magneto-Rheological Brake with Promising Environmental Performance Compared to Conventional Disc Brake

Flavio Calvi ^{1,*}, Antonella Accardo ^{1,*} , Henrique de Carvalho Pinheiro ² , Giovanni Imberti ², Ezio Spessa ¹ 
and Massimiliana Carello ² 

¹ Department of Energy G. Ferraris (DENERG), Polytechnic of Turin, Corso Duca degli Abruzzi, 24, 10129 Turin, Italy; ezio.spessa@polito.it

² Department of Mechanical and Aerospace Engineering (DIMEAS), Polytechnic of Turin, Corso Duca degli Abruzzi, 24, 10129 Turin, Italy; henrique.decarvalho@polito.it (H.d.C.P.); giovanni.imberti@polito.it (G.I.); massimiliana.carello@polito.it (M.C.)

* Correspondence: flavio.calvi@polito.it (F.C.); antonella.accardo@polito.it (A.A.)

Abstract

The European Union is currently focused on reducing non-exhaust emissions (NEE), a growing source of particulate matter (PM) pollution from road transport. This study presents the Life Cycle Assessment (LCA) of an innovative zero-emission magneto-rheological braking system specifically designed to meet new brake emission targets. Prototyped for A-segment passenger cars, the system uses magnetorheological fluids that modify their rheological properties when subjected to an external magnetic field. The environmental impacts of this innovative system are compared with those of a conventional disc brake, considering 16 environmental indicators across all life stages: raw material extraction, manufacturing, use, and end-of-life. In fact, although the system eliminates PM emissions during operation, it is crucial to assess whether it remains advantageous in terms of overall environmental impacts when the full life cycle is considered. As a prototype, this study also aims to inform design improvements that minimize environmental burdens. Results show that the innovative braking system performs better, particularly during the use and maintenance phases. Moreover, several eco-design strategies have been identified to reduce impacts related to materials and production. Overall, the magneto-rheological system demonstrates strong potential to meet future emission standards while improving the sustainability of vehicle braking technology.

Keywords: Life Cycle Assessment (LCA); magnetorheological fluid; automotive; brake; non-exhaust emissions (NEE)



Academic Editor: Michael Fowler

Received: 20 February 2026

Revised: 10 April 2026

Accepted: 16 April 2026

Published: 21 April 2026

Copyright: © 2026 by the authors.

Published by MDPI on behalf of the World Electric Vehicle Association.

Licensee MDPI, Basel, Switzerland.

This article is an open access article distributed under the terms and

conditions of the [Creative Commons Attribution \(CC BY\)](https://creativecommons.org/licenses/by/4.0/) license.

1. Introduction

The European Union is currently focused on reducing non-exhaust emissions (NEE), which are a growing source of particulate matter (PM) pollution from road transport. These emissions, which originate mainly from abrasion processes such as tire, brake, and clutch, as well as from the resuspension of deposited road dust, are becoming a larger proportion of overall PM emissions as exhaust emissions decrease. While exhaust particles have been extensively studied and successfully reduced through technological improvements, non-exhaust emissions remain less understood, with important uncertainties regarding their physicochemical properties, emission factors, and potential health impacts. Controlling

these emissions is of paramount importance, particularly because the braking system alone accounts for a significant portion between 16% and 55% by mass of total PM_x emissions from traffic on urban roads, where braking events are more frequent [1]. The EU is addressing NEE through revisions to Euro standards, particularly Euro 7, which includes measures to limit brake dust and tire wear, but achieving this goal will also require further technological improvements [2].

Recent research has investigated strategies to reduce particulate emissions from braking systems, with a primary focus on material innovations. The Lowbrasys project [3] introduced novel brake pad and disc materials. From a life cycle perspective, this new brake technology achieves a substantial 9% reduction in PM_{2.5} emissions compared to conventional disc brakes [4]. Carbon ceramic brakes are a promising solution thanks to their great properties, particularly the high wear resistance of C/SiC components. A comparative Life cycle assessment (LCA) demonstrates that traditional cast iron brakes are the more sustainable option, but conversely, the high wear resistance of composite components would result in a significant reduction in NEE PM_x [5]. While these approaches significantly decrease brake wear particles, they do not completely eliminate them, leaving room for further innovation. In this context, the development of zero-emission braking systems represents a significant step forward.

To address NEE, particularly the formation of PM_x from braking systems, several technologies have been developed and are already available on the market, representing the current state of the art. These include hysteresis brakes, eddy-current brakes, magnetic particle brakes, and magneto-rheological (MR) brakes.

Hysteresis brakes generate braking torque through magnetic hysteresis in ferromagnetic materials across an air gap rather than through frictional contact. As a result, they are intrinsically low-wear and avoid tribological particulate generation associated with conventional friction interfaces. Hysteresis-based devices are also known for smooth torque and low-noise operation; however, their low torque density limits their suitability for high-torque automotive braking applications [6–8].

Magnetic particle brakes generate braking torque by applying a magnetic field that structures the powder in the working gap between rotating members. Their torque can be regulated through the excitation current, but their behavior exhibits hysteresis and speed dependence. In addition, limited torque-transmission capacity and heat generation under operating conditions make their implementation in vehicle driveline applications challenging [9,10].

Eddy-current brakes operate by inducing currents in a conductive disc and converting kinetic energy into thermal energy without mechanical friction. While this technology performs well at high speed, its braking torque decreases significantly at low speed and remains below the level typically required for passenger vehicles, making it more suitable for applications such as high-speed rail [11–13].

Among these, MR brakes offer a particularly promising solution. This braking technology is the most suitable for the application, as it can achieve torque comparable to traditional disc brakes [14]. However, an innovative geometry is needed to optimize torque and control temperature, ensuring consistent braking performance [15]. By relying on controllable fluid dynamics rather than direct friction, MR brakes avoid the production of brake dust, demonstrating in this way promising environmental performance over traditional brake systems. In the rapidly growing field of electric vehicles (EVs), this system offers strong integration potential and benefits in reducing non-exhaust emissions (NEE). Since electric cars are generally heavier than conventional internal combustion vehicles, traditional braking systems would otherwise generate greater amounts of brake dust.

In order to better understand the environmental benefits that this new zero-emission braking system could bring to the EV sector, a detailed analysis using the LCA methodology is required. In the field of LCA of EVs, the literature has so far mainly focused on other aspects such as batteries [16], fuel cells [17], electric motors [18,19], permanent magnets [20], and complete vehicles [21].

Recent literature shows a growing research interest in magnetorheological braking systems, particularly in relation to structural configurations, braking performance, heat dissipation, and fluid durability [22–24]. These studies highlight the technological potential of MR brakes and the ongoing efforts to improve their functional reliability and performance. Nevertheless, to the authors' knowledge, no previous study has conducted an LCA of a zero-emission MR braking system with the aim of comprehensively evaluating its environmental impacts and explicitly addressing the trade-offs associated with this promising technology. Therefore, the novelty of this study lies in the comparative LCA of an innovative MR zero-emission brake (developed at the Polytechnic of Turin) against a conventional disc brake, covering multiple environmental impact categories across the main life cycle stages. Beyond assessing its overall environmental performance, the study also aims to identify the most critical impact hotspots and trade-offs of the current prototype and to provide actionable guidance for future design improvements. This integrated solution, known as the zero-emission driving system (ZEDS), combines the in-wheel motor (IWM) and braking functions, representing the evolution of traditional MR brakes while introducing a novel approach to zero-emission mobility. The work focuses in particular on the zero-emission braking functionality, evaluating its environmental performance and its potential for impact reduction compared to a traditional braking system.

2. Materials and Methods

This study follows the LCA methodology in compliance to ISO standards and reference books [25–28]. The analysis consists of 4 main steps, assessed in the successive sections: Goal and scope Section 2.2, Life Cycle Inventory Section 2.3, Life Cycle Impact Assessment Section 2.4 and finally the Results and Interpretation Section 3 part.

To carry out this study, the SimaPro 9.3.0.3 software was used, which allows the environmental impact across various production and operational processes to be assessed using the Ecoinvent database.

2.1. Case Study

The case study of this analysis is the ZEDS developed by the Polytechnic of Turin (PoliTo), which represents an innovative evolution of MR brakes [14,15]. Conceived as a project that aims to provide an integrated solution for sustainable mobility, ZEDS combines technological innovation with a broader vision of zero-emission transport. In this context, the present LCA focuses in particular on the braking functionality, which is based on a magneto-rheological fluid (MRF) that modifies its viscosity and yield strength under the effect of a magnetic field, enabling frictionless braking and eliminating PMx emissions [29]. For this reason, we will henceforth refer to the system as the zero-emission brake.

To evaluate the environmental superiority of this innovative zero emission brake, the disc brake system of a Fiat Panda (169) was selected as the baseline traditional brake technology.

The zero-emission brake investigated in this study has a substantially higher mass than the reference conventional brake system, which affects the comparison particularly in material- and manufacturing-related impact categories. This mass difference is primarily attributable to the prototype-stage architecture of the system. Unlike a conventional friction brake, the proposed design incorporates additional electromagnetic and structural

components (including the rotor, stator, copper coils, and a sealed chamber geometry designed to contain the MRF) each requiring dedicated sealing elements to prevent leakage during operation. As the current design represents a first-generation prototype rather than a production-optimized system, these components were conservatively dimensioned, resulting in a higher overall mass. The results should therefore be interpreted in light of the system's prototype-stage maturity. The current design has not yet been optimized for mass reduction, material efficiency, manufacturability, or industrial-scale production. The conservative sizing of structural and electromagnetic components, the high copper content, and the absence of a production-ready architecture are the primary drivers of the elevated environmental burdens observed in the raw material extraction and manufacturing phases. Accordingly, this assessment reflects the characteristics of an early-stage prototype rather than those of a mature, market-ready braking system.

2.2. Goal and Scope

The goal of the analysis is to evaluate the effectiveness of the innovative zero-emission brake in reducing emissions. This will be achieved by comparing it with a traditional brake system selected as a baseline. The innovative system has been shown to be effective in reducing non-exhaust PM_x emissions during its use phase. However, it is necessary to ascertain whether it remains equally effective when compared to a traditional brake in the remaining parts of the life cycle.

2.2.1. Functional Unit

In order to facilitate the comparison between the two technologies, the selected Functional Unit is "One zero emission Brake System used along 10 years, corresponding to 100,000 km (approximately 300 h of braking), suitable for a European vehicle of 800 kg". This approach was adopted in order to limit the analysis to a Single Front Brake Corner in the useful life of an average vehicle.

2.2.2. System Boundary

The System Boundary selected for this study is a cradle-to-grave (Raw Material, Manufacturing, Distribution Phase, and End of life) so it includes all stages of the brake system as represented in the Figure 1.

As shown in Figure 1, the IWM is excluded from the system boundary, so that form the analysis. This is because, from the perspective of a Comparative LCA, the architecture upstream of the brake is assumed to be identical across all systems and therefore irrelevant for the analysis.

2.3. Life Cycle Inventory

To carry out the Life Cycle Inventory (LCI) phase, the background datasets from Ecoinvent 3.0 are used. When a process unit was not available in Ecoinvent, to fill the gap, ex novo datasets were created based on secondary data available in the literature. This is the case for the dataset related to the production of the MRF, the main component of the proposed system.

All the required data for the LCI of zero-emission brakes come from PoliTo. These include the Bill-of-Materials (BoM) and manufacturing processes, as well as the maintenance during its lifetime. In contrast, the traditional system required input from an expert and a comprehensive literature review to gather all the necessary data.

In the following sections the main assumptions made during the development of the LCI models are provided for each life cycle phase.

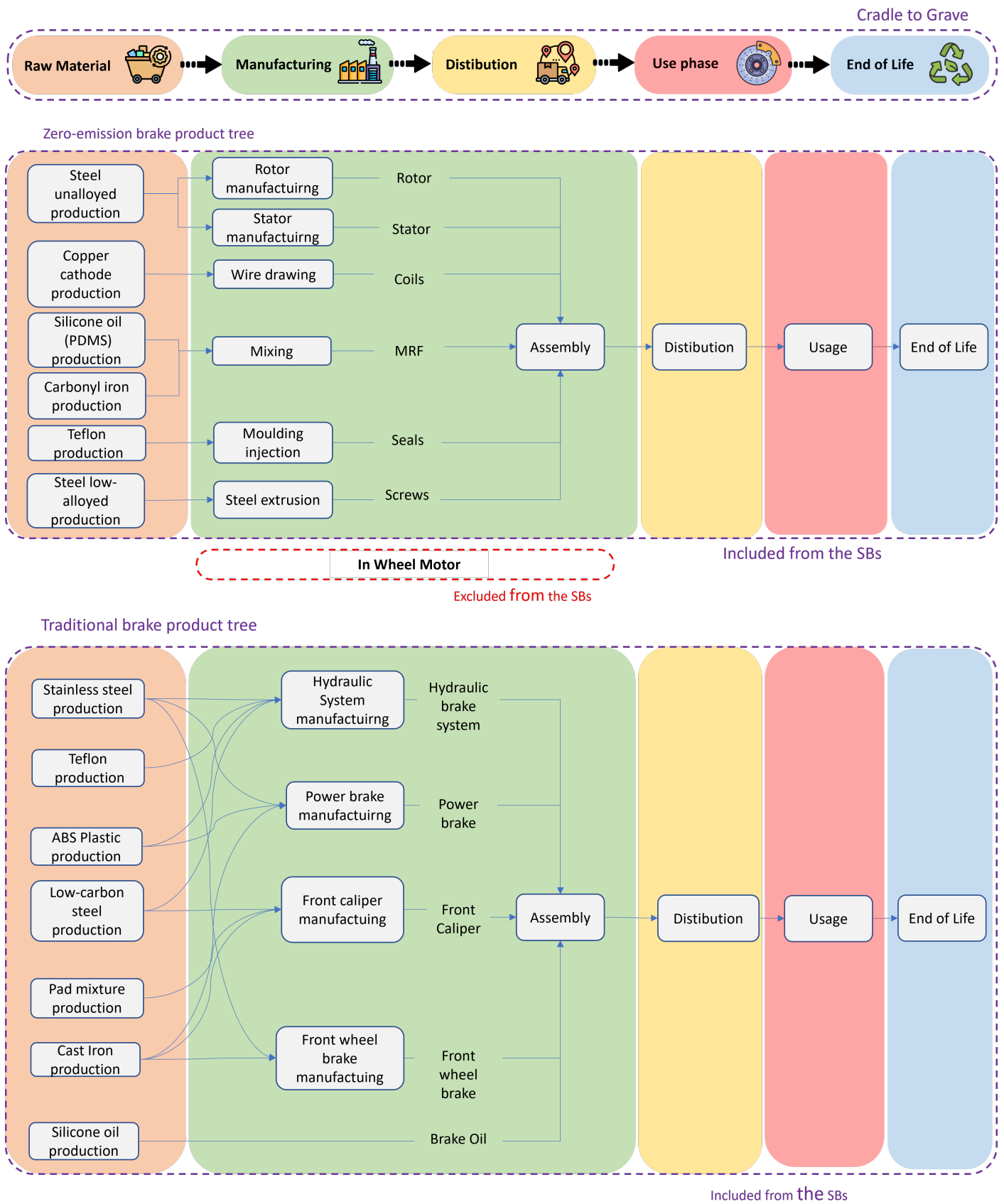


Figure 1. System boundary.

2.3.1. Raw Material

The zero-emission brake was in its early design stage, so the BoM and weights of each component are representative of the first prototype. Furthermore, since it is impossible to ascertain a precise supply chain of each material for both technologies, global average data from Ecoinvent was used as a proxy for the production and transportation from the supplier location to the manufacturing plant.

All selected materials for both products under study can be simulated using existing Ecoinvent datasets. Only two new datasets were created from scratch: the MRF for the ZEDS and the Brake Pad for the traditional brake.

The MRF is a biphasic fluid of low-viscosity silicone oil and carbonyl iron powder [30]. Table 1 reports the BoM for the MRF employed in the zero-emission brake, including the constituent materials and their quantitative proportions [31]. It was broken down into a biphasic mixture of Polydimethylsiloxane (PDMS), which represents the commonly employed carrier fluid [32], and an iron pellet selected as a proxy to represent carbonyl iron, as it is a fine spherical powder consisting essentially of high-purity elemental iron [30].

Table 1. MRF BoM and dataset.

Volume [mL]	Composition %wt	Material
300	80% Carbonyl Iron 20% Silicone Oil	Iron Pellet PDMS
MRF Density	3 g/cm ³ [31]	

Brake pads are commonly made of a composite material accurately selected to achieve the required friction properties [33]. Since the exact composition of the reference brake pad could not be obtained from the manufacturer, a custom composition was developed from scratch following the recipe in Table 2, based on common compositions reported in the literature [33,34]. This assumption introduces uncertainty into the assessment, since brake pad composition can significantly influence particulate wear emissions and toxicity-related impact categories [35,36]. Therefore, the results for impact categories that are particularly sensitive to pad formulation should be interpreted with caution.

Table 2. Brake pad recipe.

Material	Content (%wt)
Phenolic Resin	20%
Calcium Carbonate	40%
Graphite	10%
Glass Fiber	20%
Alumina	10%

2.3.2. Manufacturing and Distribution

The majority of the mechanical processes involved in the production of both brake systems are already covered by the Ecoinvent database. However, a key manufacturing process involved in the realization of several components of the traditional system is the casting process, which is unfortunately not included in the database for cast iron and steel. As a result, it was necessary to create an ex-novo dataset. This dataset was developed using relevant information already present in the Ecoinvent database, supplemented by a literature review on sand casting [37–41], which was selected as a representative method for this manufacturing stage.

The distribution of both manufactured and assembled products on the market was modeled statistically. To evaluate these transports, a weighted average distance was calculated between Turin (PoliTo was assumed as OEM) and the 10 European countries with the highest vehicle production in 2023, with the weights corresponding to the number of vehicles produced in each country [42].

2.3.3. Use Phase

In accordance with the FU selected in the Section 2.2.1, the Use Phase of both products was evaluated in relation to the life time of 100,000 km [24].

As the zero-emission brake is a frictionless system, no NEE emissions occur. Therefore, the only assumptions in this life phase concern standard maintenance work, consisting of the following:

- Replacing the MRF once over the entire service life;
- Replacing the seals once over the entire service life.

Furthermore, the electrical energy required to power the coils during operation was excluded from the present LCA. A preliminary estimate is currently available, indicating an average braking power of approximately 1 kW over an average braking time of 5 s. Nevertheless, this value refers to the current prototype stage and remains currently non-representative of the actual use-phase energy demand, as both the brake architecture and the control strategy are still under development. Since the final operational consumption will depend on future design and control refinements, the available estimate was considered too preliminary to be reliably included in the inventory model and was therefore excluded from the current analysis to avoid introducing a highly uncertain parameter that could lead to misleading comparative results. This methodological choice is in line with the literature on LCA of emerging technologies, which highlights that early-stage operational parameters are often too uncertain and non-representative to be robustly included in the inventory model before the system reaches a more stable design configuration [43–46].

In contrast, disc brakes emit PM_x as NEE. It has been estimated that the average emission factor of PM_x is 7–18.5 mg/km for PM₁₀ and 2.3–3 mg/km for PM_{2.5} per vehicle [1]. This must be replicated in the SimaPro software by creating a specific model. The worst-case scenario is used.

Maintenance of the traditional system is included. Relative assumptions are based on the vehicle maintenance plan [47]:

- The disc brake pads should be replaced every 25,000 km;
- The discs should be replaced every 50,000 km;
- The brake oil must be changed every 60,000 km.

2.3.4. End of Life

To model the EoL phase of both the zero-emission brake and the conventional disc brake, a common treatment chain was assumed, followed by material-specific recycling routes. Collection and recycling efficiencies were introduced for each material where possible, while the remaining non-recycled fraction was assumed to be treated through municipal solid waste.

First, both systems were assumed to undergo manual dismantling, in order to represent the removal of the brake assembly and the preliminary separation of its main components, followed by a shredding process for size reduction and the generation of recyclable metallic fractions. These stages were modeled using existing datasets available in the ecoinvent database, adopted as suitable proxies for component removal, shredding, and separation of the material fractions.

The subsequent pre-treatment stage, including sorting and pressing, as well as the recycling processes of steel and copper, were also modeled using existingecoinvent datasets. For steel, the EoL modeling was based on a collection rate of 0.926 and a recycling rate of 0.88, assuming recycling via electric arc furnace, resulting in an overall process rate of 0.81 [48,49]. For copper, recovered mainly from the coils of the zero-emission brake, recycling was modeled using a collection rate of 0.67 and a recycling rate of 0.63, corresponding to an overall process rate of 0.40 [48,50].

Since no suitable EoL dataset for MRFs was available in the Ecoinvent database, the treatment of the spent MRF was modeled through a newly defined process combining solid recovery and fluid re-refining. The proposed scenario consisted of two stages: (i) magnetic separation for the recovery of the iron-based particulate phase, and (ii) oil regeneration by re-refining, represented through solvent extraction and/or vacuum distillation.

(i) Carbonyl iron particles (CIP) are reported to be readily recyclable [51], and more recent studies have shown that recovered CIP can retain high magnetic responsiveness and can be effectively re-dispersed and stabilized in magnetorheological slurries, supporting their technical suitability for magnetic separation [52]. However, no study was identified reporting a specific EoL recovery rate for CIP from spent MRFs. Therefore, the 95% recovery rate adopted in this work should be regarded as a modeling assumption rather than an experimentally established value. (ii) By contrast, the recovery of the liquid phase was based on the re-refining literature for used lubricating oils, where yields of approximately 78% for solvent extraction and 84% for vacuum distillation have been reported. Accordingly, a representative base-oil recovery efficiency of 80% was assumed [53].

The energy demand associated with MRF recycling was estimated by considering the two recovery stages separately. For the re-refining stage, an LCA study on the treatment of used lubricating oils by extraction and distillation reported a cumulative energy demand of 6.144 MJ kg⁻¹ of treated oil, with distillation identified as the main energy hotspot because of its thermal requirements [54]. For the magnetic separation stage, direct data specifically referring to spent MRFs were not available. As an order-of-magnitude proxy, a National Renewable Energy Laboratory fact sheet on magnetic separation technology for ferrous minerals reported an energy intensity of 4.2 GWh per million tonnes of treated material, equivalent to approximately 0.015 MJ kg⁻¹ [55]. Although this value does not refer specifically to MRF recycling, it was considered a reasonable approximation for the magnetic separation step in the absence of more specific data.

On this basis, the total recycling energy demand per kilogram of spent MRF was approximated as follows:

$$E_{\text{recycling,MRF}} \approx x_{\text{oil}} \cdot 6.144 + x_{\text{cip}} \cdot 0.015 \quad (1)$$

where x_{oil} and x_{cip} denote the mass fractions of the liquid phase and the carbonyl iron particulate phase, respectively. According to Equation (1), the re-refining of the oil phase constitutes the dominant energy contribution, whereas magnetic separation represents a comparatively minor term.

2.4. Life Cycle Impact Assessment

Once all the data required to model both products has been collected, the next phase is the Life Cycle Impact Assessment (LCIA). This is the calculation phase in which all the data gathered during the LCI is used to assess the environmental impact of each system under analysis. To achieve this, the Environmental Footprint (EF) 3.0 method is used. The impact categories it comprises are summarised in the Table 3.

Table 3. Impact categories and their units.

Impact Category	Unit
Climate change	kg CO ₂ eq
Ozone depletion	kg CFC11 eq
Ionising radiation	kBq U-235 eq
Photochemical ozone formation	kg NMVOC eq
Particulate matter	disease inc.
Human toxicity, non-cancer	CTUh
Human toxicity, cancer	CTUh
Acidification	mol H ⁺ eq
Eutrophication, freshwater	kg P eq
Eutrophication, marine	kg N eq
Eutrophication, terrestrial	mol N eq
Ecotoxicity, freshwater	CTUe
Land use	Pt
Water use	m ³ depriv.
Resource use, fossils	MJ
Resource use, minerals and metals	kg Sb eq

To identify the most relevant impact categories, normalization and weighting have been applied in accordance with the Product Environmental Footprint (PEF) method developed by the European Commission [56].

3. Results

Figure 2 shows the comparison of the environmental impacts of the two systems considering the four most relevant impact categories. In addition, the categories of “ozone depletion” and “particulate matter” were added to allow for a more comprehensive understanding of the results obtained. The bar graph shows the contribution of the use phase only, comprised of the maintenance contribution for both the zero-emission brake (orange bars) and the traditional brake (purple bars), as well as the NEE contribution of PM2.5 (green bar) and PM10 (yellow bar) for the traditional brake.

According to Figure 2, the zero-emission brake exhibits lower environmental impacts in almost all impact categories analyzed, with an average reduction of 94% in the environmental impact of the use phase. The major reduction is in the “particulate matter” category, where the zero-emission brake shows a 99% impact reduction compared to a traditional system whose main contributors are NEEs of PM2.5 for 38% and PM10 for 35%. Contrarily to the general trend, in the “ozone layer depletion” category, the innovative zero-emission brake outperforms the traditional brake with an impact increase of approximately 70%. This is attributable to the methane and ethane emissions associated with the production processes of silicone-based spare parts (seals and MRF), since methane and ethane are the emissions with the highest CFC-11 eq characterization factor, based on the Environmental Footprint method documentation, which reports the CFs adopted in the EF framework and makes them available in the associated database and Excel package [56,57].

These results show that the zero-emission brake has promising environmental performance compared to a traditional system. This is due to lower maintenance requirements and a lower number of spare parts throughout the life cycle.

Figure 3 shows the cradle-to-grave environmental impact of the zero-emission brake, considering the four most relevant impact categories, to which the categories of “ozone depletion” and “particulate matter” were added, similarly to Figure 2. The bar charts highlight the contribution of the cradle-to-use (which includes raw material, manufac-

turing, distribution and use phases), represented by the purple bars, and the EoL phase, represented by the light blue bars.

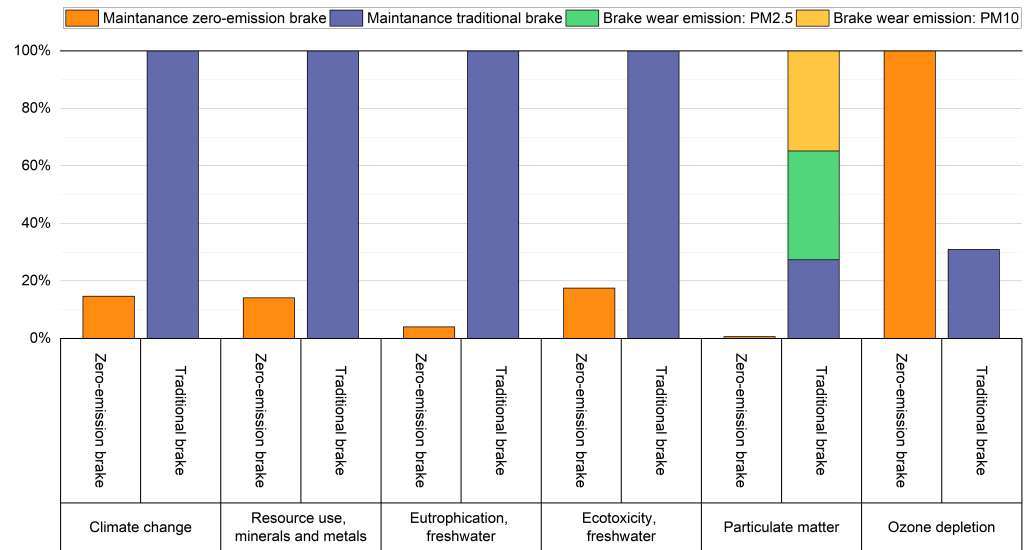


Figure 2. Comparative LCA—Use phase environmental impact comparison between the zero-emission brake and the traditional brake.

According to Figure 3, the cradle-to-use phase is the dominant contributor across all the impact categories considered. This trend is particularly evident in the categories of “climate change” and “particulate matter”, where the cradle-to-use stage accounts for more than 80% of the total impact, while the end-of-life phase plays a positive but clearly secondary role.

A different pattern can be observed for “resource use, minerals and metals”, “eutrophication, freshwater”, and “ecotoxicity, freshwater”. In these categories, the environmental burden is primarily generated during the cradle-to-use phase, whereas the end-of-life stage provides a negative contribution that offsets around 20% of the total burden generated upstream. This indicates that end-of-life management provides environmental credits that partially compensate for the impacts associated with the earlier life-cycle stages.

The most distinctive behavior is observed for the “ozone depletion” category. In this case, the credits of the end-of-life phase almost completely offset the positive impact associated with the cradle-to-use stage, leading to an overall result that is close to full compensation. This suggests that, for this specific category, the benefits related to end-of-life management are particularly significant.

Figure 4 shows a detailed cradle-to-use breakdown of the environmental impacts of the zero-emission brake. Similarly to Figure 2, the analysis considers the four most relevant impact categories, with the addition of “ozone depletion” and “particulate matter”. The bar graph highlights the contribution of each life-cycle phase within the cradle-to-use system boundary: the orange bars represent the use phase, the blue bars represent raw material acquisition, and the green and red bars represent the manufacturing and distribution phases, respectively.

According to Figure 4, the raw material acquisition and production phases have a significant impact on the product life cycle, as opposed to the use and distribution phases, which are negligible. The raw material phase has the greatest impact in the categories “Eutrophication, fresh water”, “Ecotoxicity, fresh water” and particularly in the category “Resource use, minerals and metals”, where its contribution reaches 95% of the total. In the categories “climate change” and “particulate matter”, the manufacturing phase has the greatest impact, contributing 60% and 58% respectively. In the category “ozone depletion”,

the use phase has a significant impact together with raw material acquisition, having the same contribution of about 49%.

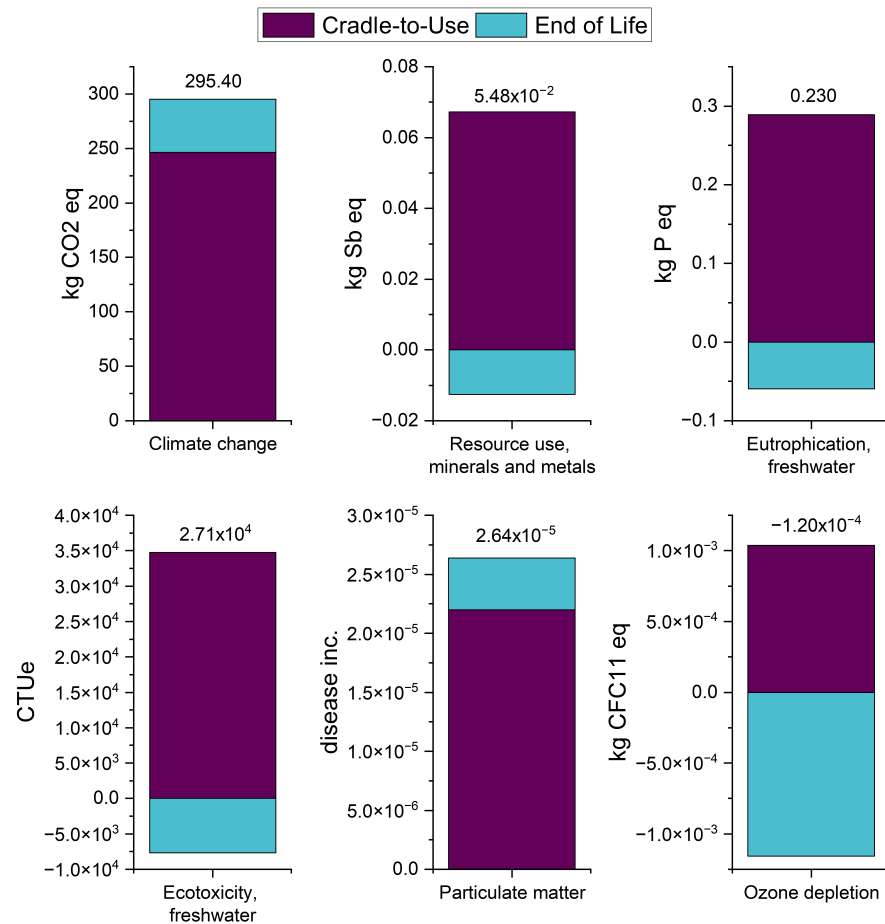


Figure 3. Zero-emission brake LCA: cradle-to-grave breakdown of the contributions of the cradle-to-use and end-of-life phases to the six environmental impact categories considered in this study. FU: One zero-emission brake system used for 10 years, corresponding to 100,000 km (approximately 300 h of braking), suitable for a European vehicle of 800 kg.

Table 4 shows the relative contribution of individual components of the braking system (namely rotor, stator, coils, seals, MRF, and others) to the six key environmental impact categories identified in this study. Absolute values for each impact category are provided in the bottom row. Coils dominate the impact in resource use and eutrophication, while the stator and rotor are more influential in climate change and particulate matter formation. Notably, seals and MRF contribute significantly to ozone depletion despite their minor role in other categories.

A more detailed analysis of the component-level contribution highlights the different roles played by the main elements of the zero-emission brake across the selected impact categories. In the case of copper coils, this significant impact is due to the process of mine extraction and refining, which are energy-intensive processes and require the use of large amounts of water, impacting the habitat and biodiversity of the area. Furthermore, the use of chemicals in the finishing and pre-processing stages can generate hazardous waste and air and water pollution. Added to this is the scarcity of copper on the planet, with few and small mines scattered around the world.

In the case of rotor and stator, this great impact on climate change is due to the energy required for the chipping process involved in the manufacturing process of these components, causing approximately 141 kg CO_{2eq} per FU.

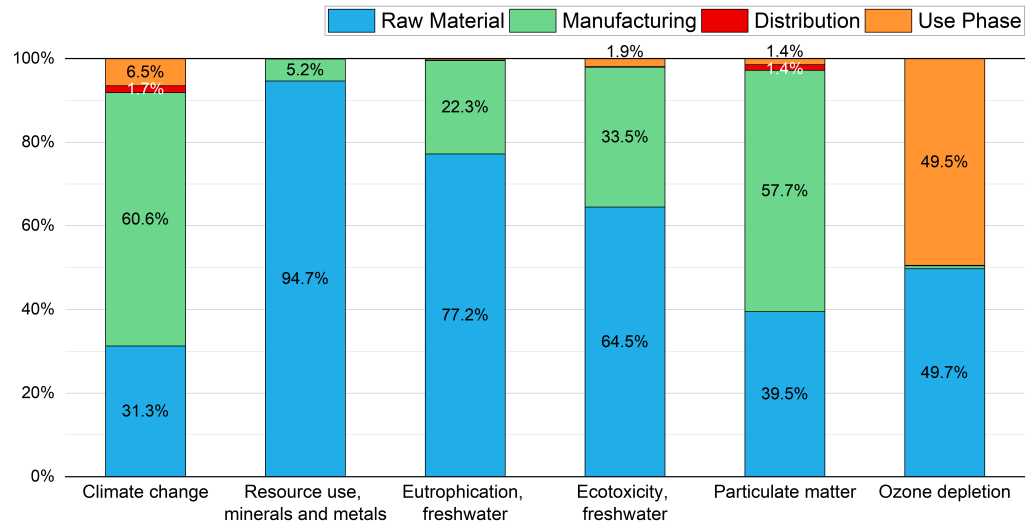


Figure 4. Zero-emission brake LCA—cradle-to-use breakdown of the life cycle phases contribution to the six key environmental impact categories identified in this study. Contributions of less than 1% are hidden.

Table 4. Zero-emission brake LCA—relative contribution of individual components of the braking system to the six key environmental impact categories identified in this study. FU: One zero-emission brake system used for 10 years, corresponding to 100,000 km (approximately 300 h of braking), suitable for a European vehicle of 800 kg.

Component	Resource Use, Minerals and Metals (kg Sb eq)	Climate Change (kg CO ₂ eq)	Eutrophication Freshwater (kg P eq)	Ecotoxicity Freshwater (CTUe)	Particulate Matter (disease inc.)	Ozone Depletion (kg CFC11 eq)
Rotor	0.71%	31.79%	10.42%	15.01%	29.66%	0.37%
Stator	0.83%	37.09%	12.16%	17.51%	34.60%	0.43%
Coils	98.18%	15.40%	76.29%	63.21%	30.45%	0.19%
Seals	0.09%	10.36%	0.23%	0.15%	0.42%	61.13%
MRF	0.06%	2.39%	0.46%	3.65%	2.29%	37.77%
others	0.13%	2.97%	0.43%	0.47%	2.58%	0.10%
Total	7.13×10^{-2}	239.90	0.300	3.66×10^4	2.13×10^{-5}	1.03×10^{-3}

Table 5 reports a breakdown at the component-level, highlighting the relative contribution of the raw material and manufacturing stages within the impact categories in which each component is most critical.

According to Table 5 in the case of “climate change”, the impacts associated with the rotor and stator are largely driven by manufacturing, which indicates that the environmental burden of these two structural components is mainly associated with the energy demand of the mechanical manufacturing processes rather than with steel production itself. In those categories of “resource use, minerals and metals”, “ecotoxicity, freshwater”, and “eutrophication, freshwater”, the contribution of the coils is almost entirely associated with copper raw material production. This confirms that these categories are influenced mainly by copper extraction and refining, rather than by downstream manufacturing oper-

ations. For “ozone depletion”, the contribution of seals and MRF is entirely associated with the raw material phase, namely the production of the silicone-based materials from which these components are derived. Finally, the impact on “particulate matter” is shared mainly among three components, namely rotor, stator, and coils. For the coils, the contribution is primarily linked to copper raw material production, while the contribution of rotor and stator is mainly driven by manufacturing.

Table 5. Zero-emission brake LCA—relative contribution of raw material and manufacturing phases for the main component-level hotspots in the most critical impact categories.

Impact Category	Main Component(s)	Raw Material	Manufacturing
Climate change (kg CO ₂ eq)	Rotor, Stator	14.5%	85.5%
Resource use, minerals and metals (kg Sb eq)	Coils	96.5%	3.5%
Ecotoxicity, freshwater (CTUe)	Coils	95.8%	4.2%
Eutrophication, freshwater (kg P eq)	Coils	95.8%	4.2%
Ozone depletion (kg CFC11 eq)	Seals, MRF	100%	0%
Particulate matter (disease inc.)	Coils	94.3%	5.7%
Particulate matter (disease inc.)	Rotor, Stator	13.2%	86.8%

Figure 5 compares the environmental impacts of the two braking systems across the four most relevant impact categories, with the additional inclusion of “ozone depletion” and “particulate matter”, consistently with Figures 2–4. The results are presented in two radar charts: panel A refers to the cradle-to-grave system boundary, whereas panel B refers to the cradle-to-use perspective. In both diagrams, the zero-emission brake is represented by green lines with square markers, while the traditional brake is represented by red lines with circular markers.

According to Figure 5A, from a cradle-to-grave perspective, the zero-emission brake shows a more favorable environmental performance only in the “ozone layer depletion” category, where the zero-emission brake shows a markedly lower impact than the traditional brake. In contrast, the zero-emission brake exhibits higher impacts in all the remaining categories.

According to Figure 5B, from a cradle-to-use perspective, the zero-emission brake performs better in the target categories of “climate change” and “particulate matter”, with reductions of 25% and 70%, respectively. Conversely, it shows higher impacts in the other categories.

This behavior can be mainly attributed to the different contributions of the life-cycle stages under the cradle-to-use and cradle-to-grave perspectives. Under the cradle-to-use perspective, the higher impacts of the zero-emission brake in most categories are mainly related to its greater weight and its current prototype configuration. Indeed, the zero-emission brake weighs approximately 17 kg, almost twice as much as the traditional braking system (9 kg), and this directly affects the environmental burdens associated with material demand. In addition, as a prototype, it has not yet been fully optimized in terms of bill of materials and production processes. Consequently, as shown in Figure 4, raw material extraction and manufacturing represent the most burdensome stages in its life cycle.

Under the cradle-to-grave perspective, these burdens are further amplified by the end-of-life stage. As shown in Figure 3, the end-of-life treatment of the zero-emission brake has a significant influence on all the impact categories considered. This is mainly due to the greater complexity of the system, which requires additional processing steps, the treatment and recycling of a larger amount of materials, and further energy consumption during end-of-life operations. As a result, the end-of-life stage contributes to increasing the overall

environmental burden of the zero-emission brake relative to the traditional brake, thereby helping to explain the less favorable results observed from the cradle-to-grave perspective in Figure 5A.

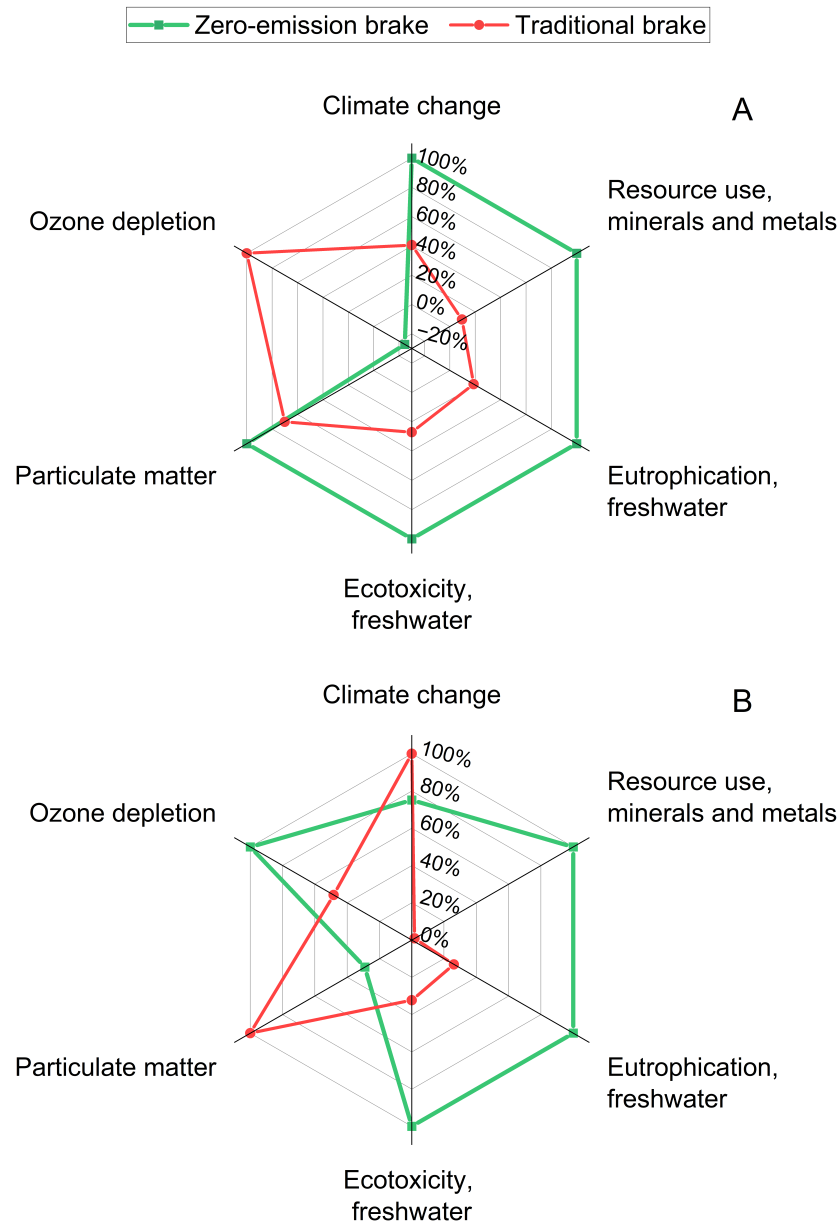


Figure 5. Comparative LCA—Life cycle environmental comparison between the zero-emission brake and the traditional brake from a (A) cradle-to-grave and (B) cradle-to-use approaches.

3.1. Sensitivity Analysis

To evaluate potential improvements of the prototype, a sensitivity assessment has been carried out based on relevant hotspots, namely the use of virgin copper and the assumed manufacturing stages. The results of the sensitivity analysis are presented from a cradle-to-use perspective to better understand variations in environmental impact and the sensitivity of the model.

Table 6 compares the environmental impacts of three scenarios: the traditional brake, the zero-emission brake prototype, and an optimized version incorporating secondary (recycled) copper. The first row lists the six evaluated impact categories. The second row presents the traditional brake results, while the third row shows the results for the zero-

emission brake with recycled copper, along with the percentage reduction in environmental impact relative to the initial prototype.

This sensitivity assessment is based on an optimization of the use of recycled copper by increasing the quantity of secondary material from scratch. This is performed by using a different dataset which considers a high recycled copper content (95%) aligned with European Union recycling directives (ELV Directive, minimum 85%) [58]. As shown in Table 6, this optimization leads to an extraordinary improvement of the zero-emission brake, reducing impacts in all categories. The most significant reductions are observed in the impact categories where virgin copper had the highest influence, as highlighted in Table 4. This substantial decrease is primarily attributed to the reduced use of virgin copper and the predominant reliance on secondary (recycled) copper. As a side effect, the sensitivity analysis also reveals improvements in the zero-emission brake's performance in both target impact categories of "climate change" and "particulate matter", further increasing its environmental advantage over the traditional brake. Furthermore, the table shows an incredible improvement of the prototype, which is now also comparable in terms of environmental impact in the remaining analyzed impact categories.

Table 6. Cradle-to-use comparison among the traditional brake, the prototype, and the optimized version of the zero-emission brake as a result of the sensitivity analysis based on the use of recycled copper.

Life Cycle	Resource Use, Minerals and Metals (kg Sb eq)	Climate Change (kg CO ₂ eq)	Eutrophication Freshwater (kg P eq)	Ecotoxicity Freshwater (CTUe)	Particulate Matter (disease inc.)	Ozone Depletion (kg CFC11 eq)
Traditional brake	1.26×10^{-3}	319.46	0.078	1.18×10^4	7.34×10^{-5}	5.00×10^{-4}
Zero-emission brake—recycled copper	2.01×10^{-3}	207.05	0.0711	1.37×10^4	1.58×10^{-5}	1.03×10^{-3}
% variation—recycled copper vs. prototype	−97.17%	−13.71%	−76.29%	−62.62%	−26.08%	−0.17%

Figure 6 shows the LCA comparison between the optimized zero-emission brake using recycled copper and the traditional brake. The assessment comprises the four most relevant impact categories, to which "ozone depletion" and "particulate matter" were added consistent with the approach adopted in Figure 5. In the radar chart, the results for the zero-emission brake with recycled copper are shown in black, while those for the traditional system are shown in red.

Complementing the tabular data, Figure 5 provides a visual representation of these improvements. According to the radar diagram, the zero-emission brake with recycled copper achieves markedly better environmental performance in three impact categories compared to the traditional brake. Reductions are particularly notable in resource use, ecotoxicity, and eutrophication, which, as illustrated in Figure 4, were previously heavily penalized by the exclusive reliance on virgin copper in the prototype version. Remarkably, these improvements have been achieved despite the system still having a considerably higher mass, demonstrating that the integration of recycled copper can substantially reduce the environmental impact of this innovative zero-emission brake.

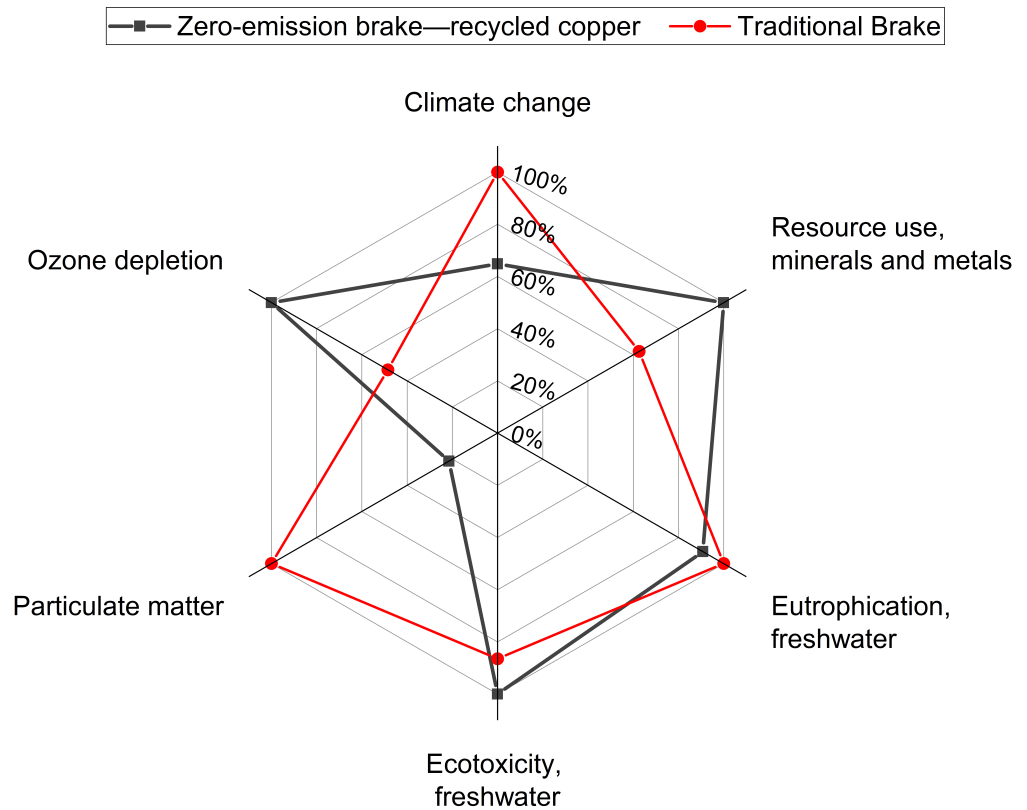


Figure 6. Comparative LCA—cradle-to-use life cycle environmental comparison between the zero-emission brake with recycled copper and the traditional brake.

Table 7 presents a comparison of the life cycle environmental impacts of the reference model, the zero-emission brake prototype, and a potential optimized model assuming an improvement of manufacturing processes. The first row lists the six evaluated impact categories. The second row presents the traditional brake results, while the third row shows the results for the zero-emission brake with recycled copper, along with the percentage reduction in environmental impact relative to the initial prototype.

This sensitivity assessment is based on the optimization of the manufacturing process, assuming large-scale production. The processes were standardized to those of the reference system, where sand casting is the predominant production method. As shown in Table 7, this optimization leads to an improvement of the zero-emission brake, reducing impacts in all categories compared to the prototype, except for “ozone reduction”. This exception is due to the fact that the optimization only applies to the rotor and stator production, while the coils and silicon-based components, which heavily influence ozone depletion, remain unchanged.

In this sensitive scenario, the zero-emission brake proves to be even more advantageous in the target categories of “climate change” and “particulate matter”. Although it performs better in other categories, it still remains less favorable compared to the traditional brake overall. Since both systems share the same production process and most of the basic materials, the key difference lies in their size and weight.

Table 7. Cradle-to-use comparison among the traditional brake, the prototype, and the optimized version of the zero-emission brake as a result of the sensitivity analysis based on an optimization of manufacturing processes.

Life Cycle	Resource Use, Minerals and Metals (kg Sb eq)	Climate Change (kg CO ₂ eq)	Eutrophication Freshwater (kg P eq)	Ecotoxicity Freshwater (CTUe)	Particulate Matter (disease inc.)	Ozone Depletion (kg CFC11 eq)
Traditional brake	1.26×10^{-3}	319.46	0.078	1.18×10^4	7.34×10^{-5}	5.00×10^{-4}
Zero-emission brake— <i>optimized manufacturing</i>	7.05×10^{-2}	175.30	0.273	3.10×10^4	1.60×10^{-5}	1.03×10^{-3}
% variation—optimized manufacturing vs. prototype	−1.12%	−26.92%	−9.00%	−15.30%	−24.88%	0.00%

Figure 7 presents the LCA comparison between the zero-emission brake with optimized manufacturing and the traditional brake. The assessment comprises the four most relevant impact categories, to which ozone depletion and particulate matter were added consistent with the approach adopted in Figure 4. In the radar chart, the results for the zero-emission brake with optimized manufacturing are shown in blue, while those for the conventional system are shown in red.

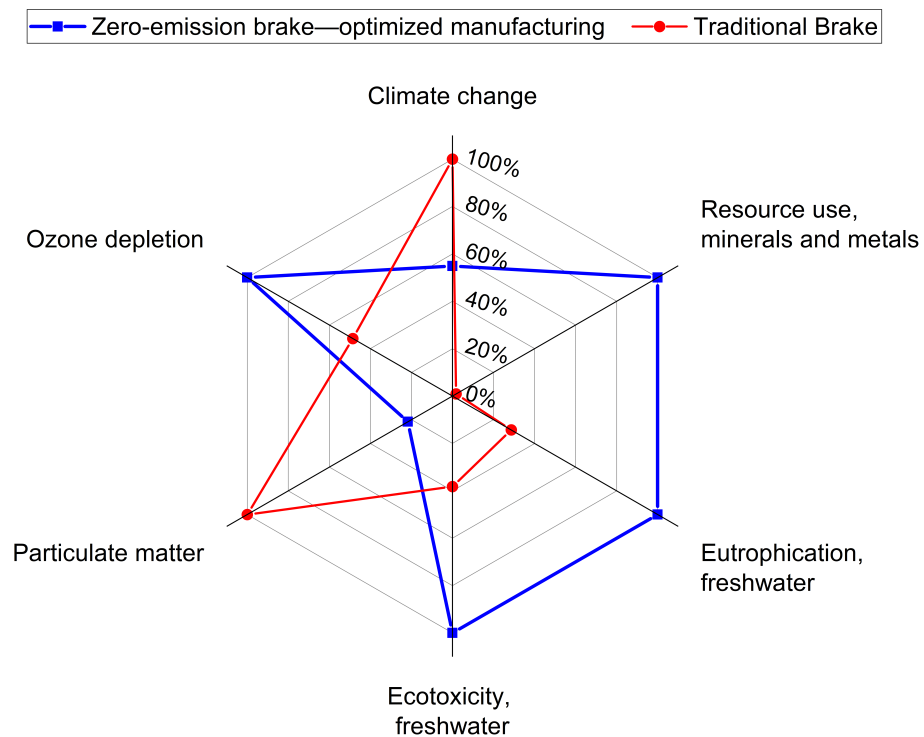


Figure 7. Comparative LCA—cradle-to-use life cycle environmental comparison between the zero-emission brake with optimized manufacturing and the traditional brake.

Complementing the tabular analysis, the radar diagram in Figure 7 visually illustrates these improvements. The optimized zero-emission brake demonstrates a marked reduction in impacts for the target categories of particulate matter and climate change, by 45% and 78%, respectively, compared to the traditional system. For the remaining categories, although the table indicates some decrease in emissions relative to the prototype, no significant variation is readily apparent.

3.2. Monte Carlo Analysis

In order to evaluate the reliability and variability of the LCA conducted in this study, a Monte Carlo analysis has been carried out to assess the effects of data and process uncertainty on the impact assessment results. The analysis is based on 10,000 iterations, a value consistent with common practice in the LCA literature, although no universally valid number of runs has been established and the appropriate choice remains case-dependent [59,60]. To interpret the uncertainty of the simulated results, different statistical indicators were considered: the standard deviation (SD) was used to describe the absolute spread outcomes around the mean, whereas the coefficient of variation (CV) was used as a dimensionless measure of relative variability, thus allowing comparison across impact categories with different magnitudes and units [61,62]. Moreover, the standard error of the mean (SEM) was used as an indicator of the numerical precision with which the Monte Carlo mean was estimated, and not as a direct measure of the variability of the simulation outcomes themselves [63].

Table 8 reports the Monte Carlo uncertainty analysis of the zero-emission brake on the cradle-to-grave perspective. The results include the mean and median values, followed by statistical indicators of SD, CV, and SEM.

According to Table 8, the Monte Carlo uncertainty analysis shows clear differences among the impact categories in terms of dispersion, relative variability, and stability of the estimated mean. The categories of “climate change” and “resource use, minerals and metals” categories the standard deviation shows the most stable and robust patterns, both categories with low SD and CV, indicating a relatively compact distribution of simulated outcomes, as well as low SEM values, suggesting that mean values are estimated with high numerical precision.

The categories of “particulate matter” and “ecotoxicity, freshwater” are characterised by higher SD and CV values than before, indicating a broader spread of Monte Carlo outcomes and a moderate degree of relative uncertainty, while their low SEM values confirmed a stable estimation of the mean. “eutrophication, freshwater” shows the highest SD and CV relative to its mean among the categories with positive mean values, indicating very high dispersion and limited robustness, despite a low SEM that only reflects the numerical precision of the estimated mean. Particular attention should be given to the “ozone depletion” category. In this case, the Monte Carlo distribution is centred close to zero, and its 95% Monte Carlo uncertainty interval spans both negative and positive values. This indicates that the sign and magnitude of the result are not robust under uncertainty, and no clear tendency toward either a positive or a negative impact can be established. The final result therefore appears to reflect a delicate balance between opposing contributions rather than a clearly dominant impact pattern. Under these conditions, the standard deviation is large relative to the mean, while the coefficient of variation loses practical interpretability because it is strongly affected by the near-zero mean. Therefore, the ozone depletion result should be interpreted with particular caution, and no strong conclusion should be drawn for this impact category.

Table 8. Monte Carlo uncertainty results for the six key environmental impact categories identified.

Statistic Indicator	Climate Change (kg CO ₂ eq)	Resource Use, Minerals and Metals (kg Sb eq)	Eutrophication, Freshwater (kg P eq)	Ecotoxicity, Freshwater (CTUe)	Particulate Matter (disease inc.)	Ozone Depletion (kg CFC11 eq)
Mean	296.95	5.48×10^{-2}	0.23	2.73×10^4	2.64×10^{-5}	-1.18×10^{-4}
Median	295.90	5.45×10^{-2}	0.23	2.66×10^4	2.59×10^{-5}	-1.27×10^{-4}
SD	16.06	3.06×10^{-3}	0.10	5.39×10^3	3.55×10^{-6}	1.04×10^{-4}
SEM	0.16	3.06×10^{-5}	9.95×10^{-4}	5.39×10^1	3.55×10^{-8}	1.04×10^{-6}
CV (%)	5.41	5.59	42.41	19.78	13.47	-87.69

Figure 8 shows the cradle-to-grave LCA results of environmental impacts of the two analyzed systems across the six key environmental impact categories identified in this study. The bar chart reports the environmental impact of the zero-emission brake with orange bars and the contribution of the traditional brake with purple bars. The impacts were normalized to the highest score in each category. The vertical error bars indicate the uncertainty associated with each result and represent an approximate 95% uncertainty range.

As illustrated in Figure 8 and supported by the Monte Carlo results, the zero-emission brake consistently showed a lower impact than the conventional brake in the ozone depletion category, with this outcome occurring in 100% of the simulations. By contrast, in all the remaining impact categories, the zero-emission brake consistently exhibited higher impacts than the traditional brake across 100% of the Monte Carlo runs.

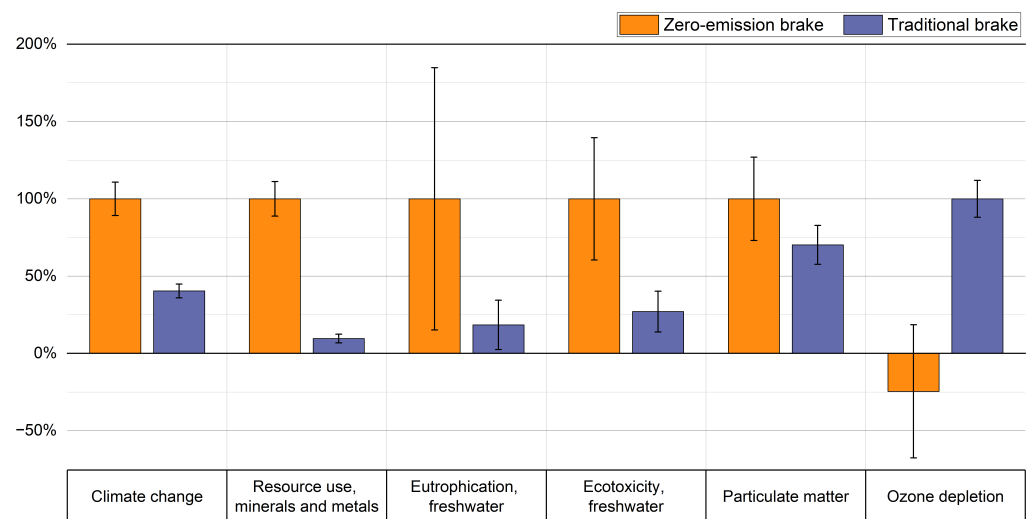


Figure 8. Comparative LCA—cradle-to-grave life cycle environmental comparison between the zero-emission brake and the traditional brake with 95% uncertainty range (calculated as $\pm 2 \times SD$).

4. Conclusions

The objective of this study is to evaluate the environmental performance of an innovative zero-emission brake through a Life Cycle analysis, comparing it with a traditional

braking system to determine whether the proposed solution offers advantages throughout its entire life cycle.

The results revealed that the zero-emission brake offers significant benefits during the use phase, mainly due to the elimination of particulate emissions as a result of the frictionless nature of the system, and a reduction in maintenance by more than 50%, resulting in a lower environmental impact from the production of spare parts.

However, the system shows clear disadvantages in the raw material and manufacturing phases, mainly due to the use of copper and to the substantially higher mass of the current prototype (approximately 17 kg versus 9 kg for the conventional system). This mass difference is one of the main factors driving the higher environmental burdens outside the use phase. A sensitivity analysis, incorporating more efficient mass-production techniques such as sand casting, confirmed that while some improvements can be made, the elevated weight remains the principal factor contributing to the system's overall environmental burden. The uncertainty analysis using the Monte Carlo method confirmed that the study's results are stable and reliable across almost all impact categories, with particular attention for ozone depletion, whose result remains sensitive to uncertainty and should therefore be interpreted with caution. Furthermore, the uncertainty analysis confirmed that the study's comparative results are robust across all impact categories.

Despite these limitations, the study demonstrated the strong potential of the zero-emission brake in delivering effective braking performance and eliminating particulate emissions during use. Moreover, the LCA model developed in this work serves not as a definitive assessment but as a solid foundation for future iterations, allowing for continued refinement of both the environmental model and the brake system itself.

Future developments of the proposed braking system should address the optimization of the current prototype in terms of layout, mass, and geometry, with the objective of achieving a more compact and lightweight design in the next stages of development. In this context, the present study provides a valuable basis for supporting these future iterations, as it identifies the main environmental hotspots and the components that should be prioritized in the eco-design process. From a performance standpoint, although numerical simulations have shown that the braking concept is functional, experimental validation through vehicle-level application remains necessary in order to assess its actual behavior under real operating conditions.

Moreover, a further priority for future development of the LCA model will be the inclusion of the brake's operational electricity consumption in the LCA model, once the system has been validated under real vehicle operating conditions and its functioning has been optimized. This will make it possible to represent the use-phase energy demand more realistically and to further improve the robustness of the environmental assessment.

Author Contributions: Conceptualization, E.S. and M.C.; Methodology, F.C., E.S. and M.C.; Writing—original draft preparation, F.C.; investigation, F.C.; writing—review and editing, A.A., H.d.C.P., G.I., E.S. and M.C.; supervision, A.A., H.d.C.P., G.I., E.S. and M.C.; resources, A.A., H.d.C.P. and G.I. All authors have read and agreed to the published version of the manuscript.

Funding: No funding was received for this research.

Data Availability Statement: The data presented in this study are available on request from the corresponding author due to the nature of the research and commercial support; the data are not publicly available.

Acknowledgments: This work was performed at the interdepartmental Center for Automotive Research and Sustainable mobility (CARS) of Polytechnic of Turin (Italy).

Conflicts of Interest: The authors declare no conflicts of interest.

References

1. Piscitello, A.; Sethi, R.; Bianco, C.; Casasso, A. Non-exhaust traffic emissions: Sources, characterization, and mitigation measures. *Sci. Total Environ.* **2021**, *766*, 144440. [CrossRef] [PubMed]
2. Samaras, Z.C.; Kontses, A.; Dimaratos, A.; Kontses, D.; Balazs, A.; Hausberger, S.; Ntziachristos, L.; Andersson, J.; Ligterink, N.; Aakko-Saksa, P.; et al. A European Regulatory Perspective towards a Euro 7 Proposal. *SAE Int. J. Adv. Curr. Pract. Mobil.* **2022**, *5*, 998–1011. [CrossRef]
3. European Commission. LOWBRASYS—A LOW environmental impact BRAke SYStem. CORDIS—EU Research Results, 2015. Grant Agreement ID: 636592. Available online: <https://cordis.europa.eu/project/id/636592> (accessed on 8 September 2025).
4. Åström, A.H.; Gradin, K.T. Report on the LCA and LCCA Results Relative to the New Brake System. Project Deliverable Deliverable 6.3, CORDIS, 2019. Available online: <https://ec.europa.eu/research/participants/documents/downloadPublic?documentIds=080166e5c1f845ea&appId=PPGMS> (accessed on 8 September 2025).
5. Bianchi, I.; Forcellese, A.; Simoncini, M.; Vita, A.; Delledonne, L.; Castorani, V. Life cycle assessment of carbon ceramic matrix composite brake discs containing reclaimed prepreg scraps. *J. Clean. Prod.* **2023**, *413*, 137537. [CrossRef]
6. Gallicchio, G.; Palmieri, M.; Nardo, M.D.; Cupertino, F. Fast Torque Computation of Hysteresis Motors and Clutches Using Magneto-static Finite Element Simulation. *Energies* **2019**, *12*, 3311. [CrossRef]
7. Gao, B.; Cheng, Y.; Zhao, T.; Sun, H.; Cui, S. A Review on Analysis Methods and Research Status of Hysteresis Motor. *Energies* **2023**, *16*, 5715. [CrossRef]
8. Placid Industries. Hysteresis Brakes-Placid Industries. Available online: <https://placidindustries.com/products/brakes/hysteresis-brakes/> (accessed on 1 June 2025).
9. Warner Electric. Permanent Magnet and Magnetic Particle Clutches and Brakes -P-1316-WE, 2025. Available online: <https://www.warnerelectric.com/products/electromagnetic-brake/power-apply/variable-torque/mag-particle-brake> (accessed on 1 April 2026).
10. Placid Industries. Magnetic Particle Brakes-Placid Industries. Available online: <https://placidindustries.com/engineering-resources/how-magnetic-particle-brakes-work/> (accessed on 6 January 2025).
11. Asonja, T.O.; Ge, J.; Yang, G. Performance Evaluation of an Eddy Current-Based Vehicle Braking System Using Electromagnetic Simulation. *SSRN* **2025**, preprint. [CrossRef]
12. Putra, M.R.A.; Nizam, M.; Tjahjana, D.D.D.P. Design of eddy current brake for electric motorcycle braking system. *Int. J. Power Electron. Drive Syst. (IJPEDS)* **2021**, *12*, 41. [CrossRef]
13. Kitanov, S.; Podol'skii, A. Analysis of Eddy-Current and Magnetic Rail Brakes for High-Speed Trains. *Open Transp. J.* **2008**, *2*, 19–28. [CrossRef]
14. Imberti, G.; De Carvalho Pinheiro, H.; Carello, M. Design of an Innovative Zero-Emissions Braking System for Vehicles. In Proceedings of the 2022 International Conference on Electrical, Computer, Communications and Mechatronics Engineering (ICECCME), Male, Maldives, 16–18 November 2022; pp. 1–6. [CrossRef]
15. Pinheiro, H.D.C.; Imberti, G.; Carello, M. Pre-Design and Feasibility Analysis of a Magneto-Rheological Braking System for Electric Vehicles. In Proceedings of the WCX SAE World Congress Experience, Detroit, MI, USA, 18 April 2023. [CrossRef]
16. Dai, Q.; Kelly, J.C.; Gaines, L.; Wang, M. Life Cycle Analysis of Lithium-Ion Batteries for Automotive Applications. *Batteries* **2019**, *5*, 48. [CrossRef]
17. Gentilucci, G.; Accardo, A.; Spessa, E. Life Cycle Analysis of a PEM Fuel Cell System for Long-Haul Heavy-Duty Trucks. In *Conference on Sustainable Mobility, Catania, Italy, 18 September 2024*; SAE International: Warrendale, PA, USA, 2024. [CrossRef]
18. Nordelöf, A.; Grunditz, E.; Lundmark, S.; Tillman, A.M.; Alatalo, M.; Thiringer, T. Life cycle assessment of permanent magnet electric traction motors. *Transp. Res. Part D Transp. Environ.* **2019**, *67*, 263–274. [CrossRef]
19. de Souza, D.F.; Fong, J.; Hernandez, C.; do Carmo, C.E.M.; Lourenço, J.L.; Sauer, I.L.; Tatizawa, H.; de Almeida, A.T. Environmental impacts of electric motor technologies: Life cycle approach based on EuP Eco-Report. *Environ. Impact Assess. Rev.* **2025**, *111*, 107741. [CrossRef]
20. Accardo, A.; Costantino, T.; Spessa, E. LCA of Recycled (NdDy)FeB Permanent Magnets through Hydrogen Decrepitation. *Energies* **2024**, *17*, 908. [CrossRef]
21. Koroma, M.S.; Costa, D.; Coosemans, T.; Messagie, M. Comparative environmental assessment of a novel functionally integrated e-axle for passenger cars. *Transp. Res. Procedia* **2023**, *72*, 2457–2463. [CrossRef]
22. Wu, J.; Kong, W.; Liu, Y. Structural development of magnetorheological fluid brakes/clutches as typical transmission devices: A review. *J. Magn. Magn. Mater.* **2025**, *614*, 172697. [CrossRef]
23. Zhang, J.; Hu, G.; Cheng, Q.; Yu, L.; Zhu, W. Analysis of braking performance and heat dissipation characteristics of multi-disc magnetorheological brake with an inner water-cooling mechanism. *J. Magn. Magn. Mater.* **2024**, *604*, 172313. [CrossRef]
24. Imberti, G.; de Carvalho Pinheiro, H.; De Carlo, M.; Peruzzi, G.; Carello, M. Durability Analysis of a Magneto-Rheological Fluid for Automotive Braking System. *Designs* **2025**, *9*, 74. [CrossRef]

25. Joint Research Centre. *International Reference Life Cycle Data System (ILCD) Handbook: Framework and Requirements for Life Cycle Impact Assessment Models and Indicators*; Publications Office of the European Union: Luxembourg, 2010.
26. Joint Research Centre. *International Reference Life Cycle Data System (ILCD) Handbook: General Guide for Life Cycle Assessment: Detailed Guidance*; Publications Office of the European Union: Luxembourg, 2010.
27. *BS EN ISO 14040*; Environmental Management: Life Cycle Assessment: Principles and Framework. British Standards Institute: London, UK, 2006.
28. *BS EN ISO 14044*; Environmental Management: Life Cycle Assessment: Requirements and Guidelines, Withdrawn Ed. British Standards Institute: London, UK, 2018.
29. Zainordin, A.Z.; Abdullah, M.A.; Hudha, K. Experimental Evaluations on Braking Responses of Magnetorheological Brake. *Mech. Eng.* **2013**, *1*, 195–199.
30. BASF. BASF continues to evolve carbonyl iron powders. *Met. Powder Rep.* **1999**, *54*, 18–20. [CrossRef]
31. Lord, P. MRF-132DG Magneto-Rheological Fluid—Technical Data Sheet. Available online: [https://www.parker.com/content/dam/Parker-com/Literature/Assembly---Protection-Solutions-Division/Technical-Datasheets-\(TDS\)/Datasheet---MRF-132DG_MRFluid_DS7015.pdf](https://www.parker.com/content/dam/Parker-com/Literature/Assembly---Protection-Solutions-Division/Technical-Datasheets-(TDS)/Datasheet---MRF-132DG_MRFluid_DS7015.pdf) (accessed on 30 March 2026).
32. Kumar, J.S.; Paul, P.S.; Raghunathan, G.; Alex, D.G. A review of challenges and solutions in the preparation and use of magnetorheological fluids. *Int. J. Mech. Mater. Eng.* **2019**, *14*, 13. [CrossRef]
33. Kumar, S.; Ghosh, S.K. Particle emission of organic brake pad material: A review. *Proc. Inst. Mech. Eng. Part D J. Automob. Eng.* **2020**, *234*, 1213–1223. [CrossRef]
34. Ghazali, C.M.R.; Kamarudin, H.; Jamaludin, S.B.; Abdullah, M.M.A.B. Comparative Study on Thermal, Compressive, and Wear Properties of Palm Slag Brake Pad Composite with other Fillers. *Adv. Mater. Res.* **2011**, *328–330*, 1636–1641. [CrossRef]
35. Hoff, M.; Chen, Y.M.; Meunier, L.; Bressot, C.; Morgeneyer, M. Effect of Friction Material on Vehicle Brake Particle Emissions. *Atmosphere* **2025**, *16*, 1075. [CrossRef]
36. Varriale, F.; Carlevaris, D.; Wahlström, J.; Malmberg, V.; Lyu, Y. On the impact of pad material ingredients on particulate wear emissions from disc brakes. *Results Eng.* **2023**, *19*, 101397. [CrossRef]
37. Sappinen, T.; Peltokorpi, J.; Alieva, E.; Orkas, J. Comparison of Carbon Footprints in Sourcing of Cast Components. *Int. J. Met.* **2025**, *20*, 428–439. [CrossRef]
38. Bekker, A.C.; Verlinden, J.C. Life cycle assessment of wire + arc additive manufacturing compared to green sand casting and CNC milling in stainless steel. *J. Clean. Prod.* **2018**, *177*, 438–447. [CrossRef]
39. He, K.; Wang, L. A review of energy use and energy-efficient technologies for the iron and steel industry. *Renew. Sustain. Energy Rev.* **2017**, *70*, 1022–1039. [CrossRef]
40. Dalquist, S.; Gutowski, T. Life Cycle Analysis of Conventional Manufacturing Techniques: Sand Casting. In Proceedings of the Manufacturing Engineering and Materials Handling Engineering, Anaheim, CA, USA, 13–19 November 2004; pp. 631–641. [CrossRef]
41. Margolis, N.; Jamison, K.; Dove, L. In *Energy and Environmental Profile of the U.S. Metal Casting Industry*; Technical Report None; Energetics, Inc.: Columbia, MD, USA, 1999. [CrossRef]
42. ACEA. Economic and Market Report: Global and EU Auto Industry– Full Year 2023. 2023. Available online: <https://www.acea.auto/publication/economic-and-market-report-global-and-eu-auto-industry-full-year-2023/> (accessed on 29 October 2024).
43. Cucurachi, S.; van der Giesen, C.; Guinée, J. Ex-ante LCA of Emerging Technologies. *Procedia CIRP* **2018**, *69*, 463–468. [CrossRef]
44. Blanco, C.F.; Cucurachi, S.; Guinée, J.B.; Vijver, M.G.; Peijnenburg, W.J.G.M.; Trattig, R.; Heijungs, R. Assessing the sustainability of emerging technologies: A probabilistic LCA method applied to advanced photovoltaics. *J. Clean. Prod.* **2020**, *259*, 120968. [CrossRef]
45. Tsoy, N.; Steubing, B.; Van Der Giesen, C.; Guinée, J. Upscaling methods used in ex ante life cycle assessment of emerging technologies: A review. *Int. J. Life Cycle Assess.* **2020**, *25*, 1680–1692. [CrossRef]
46. Thonemann, N.; Schulte, A.; Maga, D. How to Conduct Prospective Life Cycle Assessment for Emerging Technologies? A Systematic Review and Methodological Guidance. *Sustainability* **2020**, *12*, 1192. [CrossRef]
47. FIAT. *Fiat Panda Owner Handbook*; FIAT: Turin, Italy, 2011. Available online: <https://www.manua.ls/ fiat/panda/manual> (accessed on 24 September 2025).
48. Accardo, A.; Spessa, E.; Martin, A.R.; Essl, J.; Duft, M.; Bachler, J. Life Cycle Assessment of Electric Drivetrains for Sustainable Transport. In Proceedings of the 2024 International Conference on Electrical Machines (ICEM), Torino, Italy, 1–4 September 2024; pp. 1–7. [CrossRef]
49. Broadbent, C. Steel’s recyclability: Demonstrating the benefits of recycling steel to achieve a circular economy. *Int. J. Life Cycle Assess.* **2016**, *21*, 1658–1665. [CrossRef]
50. International Copper Assosiation. Recycling Brief-Copper Recycling. 2022. Available online: <https://internationalcopper.org/wp-content/uploads/2022/02/ICA-RecyclingBrief-202201-A4-R2.pdf> (accessed on 4 April 2026).

51. Rabbani, Y.; Shariaty-Niassar, M.; Ebrahimi, S.A.S. The effect of superhydrophobicity of prickly shape carbonyl iron particles on the oil-water adsorption. *Ceram. Int.* **2021**, *47*, 28400–28410. [[CrossRef](#)]
52. Fang, Y.C.; Lai, C.H.; Li, C.C. Dispersion stabilization of carbonyl iron particles and its applications in chemical mechanical planarization. *Colloids Surfaces A Physicochem. Eng. Asp.* **2024**, *683*, 133003. [[CrossRef](#)]
53. Emam, E.; Shoaib, A. Re-refining of used lube oil, i- by solvent extraction and vacuum distillation followed by hydrotreating. *Pet. Coal* **2013**, *55*, 179–187.
54. Botas, J.A.; Moreno, J.; Espada, J.J.; Serrano, D.P.; Dufour, J. Recycling of used lubricating oil: Evaluation of environmental and energy performance by LCA. *Resour. Conserv. Recycl.* **2017**, *125*, 315–323. [[CrossRef](#)]
55. National Laboratory of the Rockies. *Magnetic Elutriation Technology for Clean and Efficient Processing of Iron Ore*; Technical Report DOE/GO-102001-1045; U.S. Department of Energy: Washington, DC, USA, 2001. Available online: <https://research-hub.nlr.gov/en/publications/magnetic-elutriation-technology-for-clean-and-efficient-processin/> (accessed on 1 April 2026).
56. Zampori, L.; Pant, R. *Suggestions for Updating the Product Environmental Footprint (PEF) Method*; Report No. EUR 29682 EN; JRC115959; Publications Office of the European Union: Luxembourg, 2019. [[CrossRef](#)]
57. Fazio, S.; Biganzoli, F.; Zampori, L.; Sala, S.; Diaconu, E. *Supporting Information to the Characterisation Factors of Recommended EF Life Cycle Impact Assessment Methods*; Publications Office of the European Union: Luxembourg, 2018. [[CrossRef](#)]
58. European Commission. Joint Research Centre. *Initial Analysis of Selected Measures to Improve the Circularity of Critical Raw Materials and Other Materials in Passenger Cars*; Publications Office of the European Union: Luxembourg, 2023.
59. Accardo, A.; Dotelli, G.; Musa, M.L.; Spessa, E. Life Cycle Assessment of an NMC Battery for Application to Electric Light-Duty Commercial Vehicles and Comparison with a Sodium-Nickel-Chloride Battery. *Appl. Sci.* **2021**, *11*, 1160. [[CrossRef](#)]
60. Heijungs, R. On the number of Monte Carlo runs in comparative probabilistic LCA. *Int. J. Life Cycle Assess.* **2020**, *25*, 394–402. [[CrossRef](#)]
61. Altman, D.G.; Bland, J.M. Standard deviations and standard errors. *BMJ* **2005**, *331*, 903. [[CrossRef](#)]
62. Ospina, R.; Marmolejo-Ramos, F. Performance of Some Estimators of Relative Variability. *Front. Appl. Math. Stat.* **2019**, *5*, 43. [[CrossRef](#)]
63. Sileshi, G. The Relative Standard Error as an Easy Index for Checking the Reliability of Regression Coefficients. ResearchGate. 2015. Available online: https://www.researchgate.net/publication/281371440_The_relative_standard_error_as_an_easy_index_for_checking_the_reliability_of_regression_coefficients?channel=doi&linkId=55e415b608ae2fac472143ea&showFulltext=true (accessed on 1 April 2026).

Disclaimer/Publisher’s Note: The statements, opinions and data contained in all publications are solely those of the individual author(s) and contributor(s) and not of MDPI and/or the editor(s). MDPI and/or the editor(s) disclaim responsibility for any injury to people or property resulting from any ideas, methods, instructions or products referred to in the content.